Kinetics and Modeling of Aqueous Phase Radical Homopolymerization of 3-(Methacryloylaminopropyl)trimethylammonium Chloride and its Copolymerization with Acrylic Acid

Authors:

Ikenna H. Ezenwajiaku, Emmanuel Samuel, Robin A. Hutchinson

Date Submitted: 2021-05-11

Keywords: modeling and simulation, radical polymerization, polyelectrolytes, aqueous phase polymerization

Abstract:

The radical homopolymerization kinetics of 3-(methacryloylaminopropyl) trimethylammonium chloride (MAPTAC) and its batch copolymerization with nonionized acrylic acid (AA) in aqueous solution are investigated and modeled. The drift in monomer composition is measured during copolymerization by in situ NMR over a range of initial AA molar fractions and monomer weight fractions up to 0.35 at 50 °C. The copolymer becomes enriched in MAPTAC for monomer mixtures containing up to 60 mol% MAPTAC, but is enriched in AA for MAPTAC-rich mixtures; this azeotropic behavior is dependent on initial monomer content, as electrostatic interactions from the cationic charges influence the system reactivity ratios. Models for MAPTAC homopolymerization and AA-MAPTAC copolymerization are developed to represent the rates of monomer conversion and comonomer composition drifts over the complete range of experimental conditions.

Record Type: Published Article

Submitted To: LAPSE (Living Archive for Process Systems Engineering)

Citation (overall record, always the latest version):	LAPSE:2021.0355
Citation (this specific file, latest version):	LAPSE:2021.0355-1
Citation (this specific file, this version):	LAPSE:2021.0355-1v1

DOI of Published Version: https://doi.org/10.3390/pr8111352

License: Creative Commons Attribution 4.0 International (CC BY 4.0)

processes

MDPI

Article

Kinetics and Modeling of Aqueous Phase Radical Homopolymerization of 3-(Methacryloylaminopropyl)trimethylammonium Chloride and its Copolymerization with Acrylic Acid

Ikenna H. Ezenwajiaku, Emmanuel Samuel and Robin A. Hutchinson *

Department of Chemical Engineering, Queen's University, Kingston, ON K7L3N6, Canada; ikenna.ezenwajiaku@queensu.ca (I.H.E.); emmanuel.samuel@queensu.ca (E.S.)
* Correspondence: robin.hutchinson@queensu.ca; Tel.: +1-613-533-3097

Received: 30 September 2020; Accepted: 21 October 2020; Published: 26 October 2020

Abstract: The radical homopolymerization kinetics of 3-(methacryloylaminopropyl) trimethylammonium chloride (MAPTAC) and its batch copolymerization with nonionized acrylic acid (AA) in aqueous solution are investigated and modeled. The drift in monomer composition is measured during copolymerization by in situ NMR over a range of initial AA molar fractions and monomer weight fractions up to 0.35 at 50 °C. The copolymer becomes enriched in MAPTAC for monomer mixtures containing up to 60 mol% MAPTAC, but is enriched in AA for MAPTAC-rich mixtures; this azeotropic behavior is dependent on initial monomer content, as electrostatic interactions from the cationic charges influence the system reactivity ratios. Models for MAPTAC homopolymerization and AA-MAPTAC copolymerization are developed to represent the rates of monomer conversion and comonomer composition drifts over the complete range of experimental conditions.

Keywords: aqueous phase polymerization; polyelectrolytes; radical polymerization; modeling and simulation

1. Introduction

Recent investigations have led to an improved understanding of the radical aqueous-phase polymerization kinetics of nonionized and ionizable water-soluble monomers. These water-soluble monomers are utilized to synthesize polyelectrolytes with tailor-made properties for a wide range of consumer and industrial applications such as flocculants in wastewater treatments, and personal care and pharmaceutical products [1–5]. However, monomer-solvent interactions during polymerization in aqueous phase result in complexities not encountered in organic phase, with the rate coefficients dependent on monomer concentration, ionic strength, and pH. Application of specialized techniques such as pulsed laser polymerization (PLP) used in combination with size exclusion chromatography (SEC), near infrared (NIR) spectroscopy, and electron paramagnetic resonance (EPR) spectroscopy has resulted in tremendous progress in understanding the polymerization kinetics of these water-soluble monomers [6,7].

PLP investigations have revealed that both the propagation (k_p) and termination (k_t) rate coefficients of water-soluble monomers such as methacrylic acid (MAA) [8–11] and acrylic acid (AA) [12–15] decrease with increasing monomer content in aqueous solution when the monomer is in its nonionized form, effects that have been captured in mechanistic models formulated to represent their batch and semi-batch radical homopolymerization under natural pH conditions [16–18]. Both rate coefficients decrease by orders of magnitude as pH is increased to ionize the monomer, due to the influence

of electrostatic repulsion on propagation between a charged monomer and charged radical species and on the termination between two charged radical species [10,13,19,20]. The net effect on AA polymerization is a significant decrease in the rate of monomer conversion with increasing pH; once the monomer is fully ionized, however, addition of excess salt leads to a recovery in polymerization rate [21]. This complex relationship between degree of ionization and ionic strength (through addition of salt) also greatly influences the copolymerization behavior of AA with a nonionized monomer such as acrylamide [22–25].

Similar studies of the kinetic behavior of fully ionized monomers are limited. A recent PLP-SEC investigation revealed that k_p of the permanently-charged cationic monomer 2-(methacryloyloxyethyl) trimethylammonium chloride (TMAEMC) [26] increases with increasing monomer content in aqueous solution, the opposite trend to what was observed for nonionized water-soluble monomers. This behavior was attributed to increased screening of charges on the monomer and radical structures as the concentration of counterions in solution increases. The relative influence of the charge screening on propagation and termination differs, and is influenced by various factors including the distance between the reacting radical and the location of the cationic charge. Thus, the rate of monomer conversion for TMAEMC homopolymerization was found to decrease with increased monomer content despite the increased k_p, indicating that counterion concentration has a stronger influence on the termination of charged macroradicals than propagation [27]. Polymerization rate of the permanently-charged TMAEMC remained unchanged with solution pH, demonstrating that the kinetics do not have the pH dependence found for ionizable monomers (AA and MAA). Using these observations to develop correlations for k_p and k_t as a function of solution composition, a mechanistic model for TMAEMC radical homopolymerization was developed to represent polymerization rates as well as polymer molar mass distributions (MMD) produced under a range of batch and semi-batch operating conditions [27].

Polyelectrolyte charge density and hence application properties are controlled by radical copolymerization of cationic monomers with neutral monomers such as acrylamide or ionizable monomers such as AA. While the number of studies is limited, it has been shown that the relative consumption rates of the two monomers are dependent on the initial amount of cationic monomer in the system [28–30]. Capturing these influences in mechanistic models developed to represent the polymerization system can aid selection of appropriate synthesis conditions to control the copolymer composition. Thus, the comonomer composition drifts for TMAEMC copolymerized with nonionized AA were measured using an in situ NMR technique over a range of initial compositions and monomer loadings to develop a description of how the system reactivity ratios varied as a function of aqueous solution conditions [29]. The analysis indicated that copolymer composition could be well represented using the standard model of terminal copolymerization kinetics, as long as the influence of charge-screening on TMAEMC k_p and k_t values was properly accounted for. This insight was used to develop an AA-TMAEMC copolymerization model that also included the influence of AA based midchain radicals formed through intramolecular chain transfer on reaction rates [29].

In this work, we examine whether the insights gained from the study of AA-TMAEMC copolymerization extend to similar systems. MAPTAC is an amide-based cationic monomer with a methacrylate structure similar to TMAEMC; in addition to the different functionality, the spacing between the monomer double bond and the cationic charge is increased by one CH_2 unit, as shown in Scheme 1. Given their similar structure, one would expect similarities in the influence of electrostatic interactions on the rate coefficients for these two cationic monomers and subsequently their (co)polymerization kinetics. Indeed, the recent PLP-SEC investigation revealed that increased counterion concentration (C_{Cl^-}), achieved by either increasing the initial monomer concentration or adding NaCl, increases the value of k_p for both TMAEMC and MAPTAC [26]. As shown in Figure 1, the k_p values for MAPTAC are lower than those of TMAEMC, in agreement with other comparisons of k_p values for ester vs amide-based monomers polymerized in aqueous phase [31,32]. In addition, the dependence of MAPTAC k_p on C_{Cl^-} is not as strong as that observed for TMAEMC across the entire concentration range studied, equivalent to varying the initial weight fraction of monomer in aqueous

solution ($w_{mon,0}$) between 0.05 and 0.40. This difference may be explained by reduced electrostatic effects resulting from the increased distance of the charged moiety from the reactive double bond in MAPTAC compared to TMAEMC (7 bond length vs 6 bond length) [33].

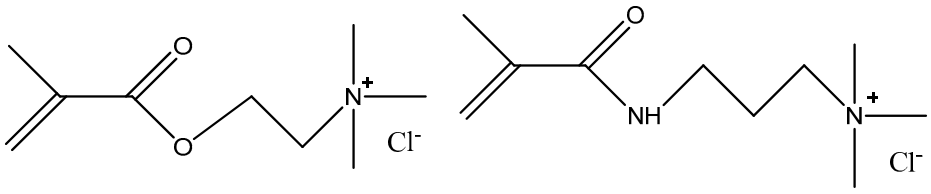

(**a**) (**b**)

Scheme 1. Structures of the cationic monomers: (**a**) 2-(methacryloyloxyethyl)trimethylammonium chloride (TMAEMC); (**b**) 3-(methacryloylaminopropyl)trimethylammonium chloride (MAPTAC).

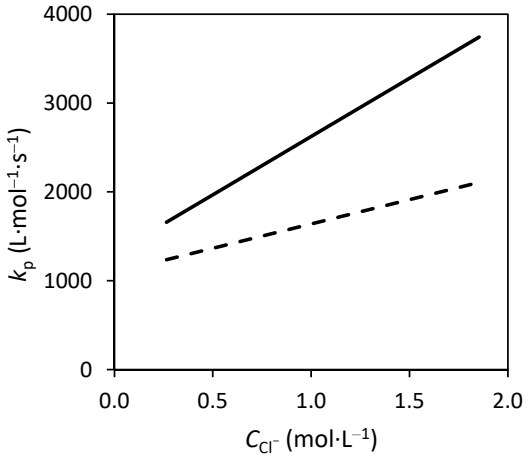

Figure 1. The dependence of k_p on counterion concentration (C_{Cl^-}) in aqueous solution for TMAEMC (—) and MAPTAC (- - -) at 50 °C, as generated using representations developed for TMAEMC [27] and MAPTAC (this work) based on PLP-SEC experimentation [26].

Under continuous initiation, a decreased rate of monomer conversion was found for both monomers when the initial monomer content was increased, with MAPTAC batch homopolymerization occurring at a lowered rate compared to TMAEMC [26]. In the present study we extend the comparison to copolymerization, applying the in situ NMR technique to investigate the influence of initial monomer composition, total monomer content ($w_{mon,0}$ between 0.05 and 0.40) and added salt (NaCl) on the copolymerization of AA-MAPTAC. The results are compared and contrasted to the recent AA-TMAEMC study conducted under a similar range of conditions [29] to provide insights on the influence of the cationic monomer structure on reactivity, and to determine whether the modeling strategy developed previously for TMAEMC homo- and copolymerization can also be used represent MAPTAC homopolymerization and its copolymerization with AA.

2. Materials and Methods

All in situ NMR experiments were carried out in deuterium oxide (D_2O, 99.9%, Cambridge Isotope Laboratories Inc., Montreal, QC, Canada) as solvent, while samples for physical measurements were prepared in deionized water. Other materials used as received from Sigma Aldrich (Oakville, ON, Canada) include: 3-(methacryloylaminopropyl)trimethylammonium chloride (MAPTAC, 50 wt% solution in H_2O), acrylic acid (AA, 99%), propionic acid (PA, ≥99.5%), sodium chloride BioXtra (NaCl, ≥99.5%, AT), sodium hydroxide reagent grade (NaOH, ≥98%, anhydrous pellets), 2,2-azobis(2-methylpropionamidine) dihydrochloride (V-50, 97%). Hydrochloric acid (HCl, reagent, ACS-PUR, Fisherbrand, Mississauga, ON, Canada) was used for adjusting solution pH. Solution

preparation for bench-scale and in situ batch polymerizations as well as the subsequent data analyses were carried out using the methods developed for the TMAEMC and AA-TMAEMC studies [27,29].

Figure 2 shows the NMR spectrum at 50 °C for an equimolar mixture of AA and MAPTAC ($f_{MAPTAC,0}$ = 0.5) with a monomer weight fraction ($w_{mon,0}$) of 0.05, and 0.80 wt% V-50 initiator in solution. The decrease in intensities of peaks from AA and MAPTAC terminal double bond protons relative to the HOD peak (4.71 ppm) was followed over time and used to calculate monomer conversion profiles and the change in the MAPTAC molar fraction, as detailed in Supporting Information. Repeat experiments carried out for AA-MAPTAC copolymerization under selected conditions showed good reproducibility, as shown in Figure S1.

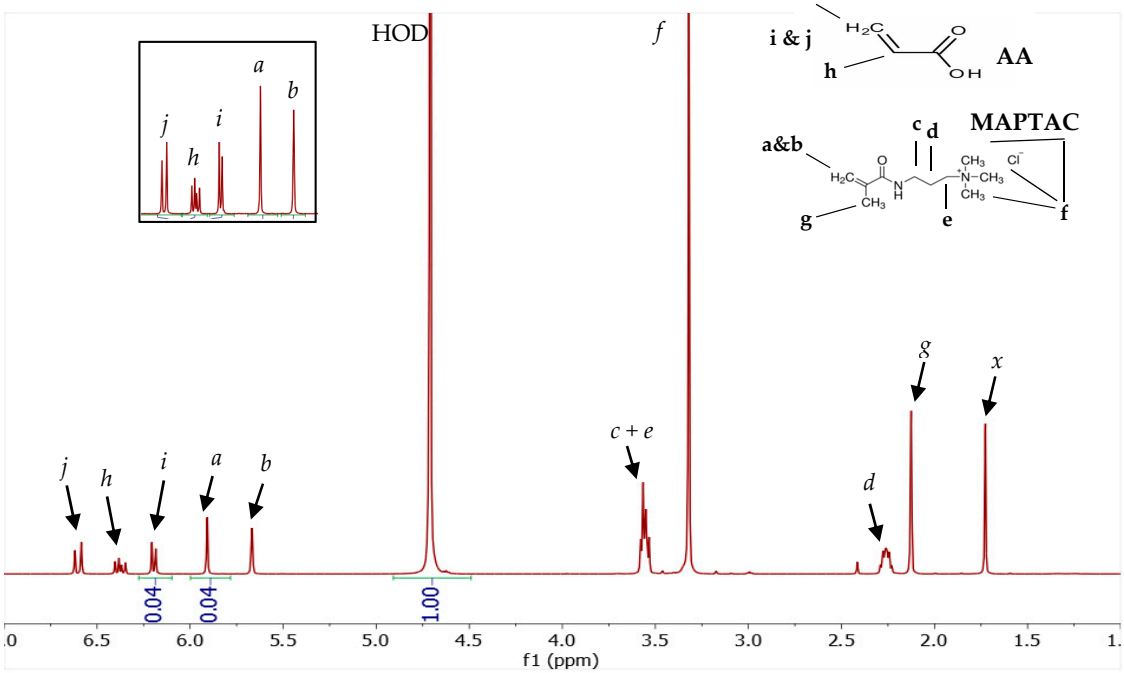

Figure 2. ^{1}H NMR peaks assignments for AA-MAPTAC comonomer mixture with $f_{MAPTAC,0}$ = 0.5, $w_{mon,0}$ = 0.05 and 0.80 wt% initiator in D_2O at 50 °C (1st scan). Peak *x* was identified as arising from V-50 initiator. Inset shows the separation of the double bond peaks used to track the relative consumption of the two monomers during reaction.

Polymer samples used for physical characterization were synthesized under the same reaction conditions with the in situ NMR method using a mixed 20 mL lab reactor, as the previous TMAEMC homopolymerization study revealed good agreement in polymer properties and reaction rates between the two techniques [27]. An Orion™ Versa Star Pro™ pH/ISE/Conductivity/Dissolved Oxygen Multiparameter Benchtop Meter was used to measure pH, and a calibrated Cannon–Fenske viscometer was utilized to obtain the dynamic viscosity of the samples.

3. Experimental Results

While there are a few investigations of the copolymerization of acrylamide with MAPTAC [5,34], no study on the copolymerization of nonionized AA with MAPTAC could be found. Thus, this section provides first results for AA-MAPTAC copolymerization, comparing them to the recent AA-TMAEMC copolymerization study [29]. Addition of AA to the MAPTAC system greatly lowers system pH to ~2 such that AA remains in its nonionized form, as it also was for copolymerization with TMAEMC [29]. Batch copolymerization experiments with $w_{mon,0}$ of 0.10 and initial MAPTAC molar fractions ($f_{MAPTAC,0}$) varied between 0.3 and 0.9 were investigated at 50 °C and 0.80 wt% V-50 in D_2O using in situ NMR to measure polymerization rates and copolymer composition. As shown by the conversion profiles in Figure 3a, the rate of polymerization systematically decreases with an increase in initial MAPTAC

fraction up to 90% mol. The polymerization rate at $f_{MAPTAC,0}$ = 0.9 matches that of MAPTAC homopolymerization, despite the significant difference in solution pH, 2.8 for $f_{MAPTAC,0}$ = 0.9 and 6.7 for MAPTAC homopolymerization, respectively. Figure 3b plots the change in f_{MAPTAC}, the molar fraction of MAPTAC remaining in the comonomer solution, as a function of conversion. MAPTAC is preferentially incorporated into the copolymer (as indicated by the decrease in f_{MAPTAC}) for the experiments conducted with $f_{MAPTAC,0}$ = 0.3 and 0.5, but there is a preferential incorporation of AA into the copolymer with $f_{MAPTAC,0}$ = 0.7 and 0.9. Initial rates could not be captured by the in situ NMR technique at the higher V-50 level used for AA-MAPTAC copolymerization with $f_{MAPTAC,0}$ = 0.10.

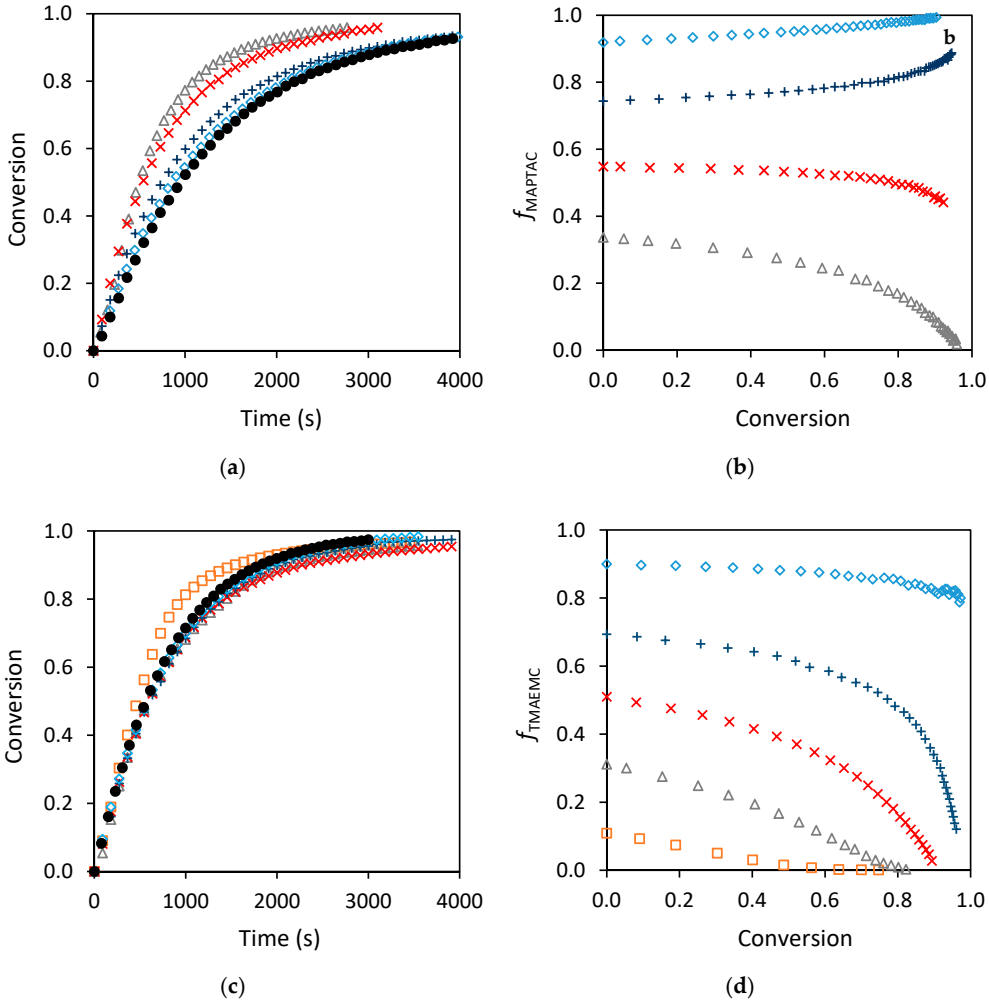

Figure 3. Overall monomer conversion profiles for (**a**) AA-MAPTAC and (**c**) AA-TMAEMC, and composition drift of (**b**) MAPTAC and (**d**) TMAEMC mole fraction when copolymerized with AA at 50 °C with 0.80 (for MAPTAC) and 0.40 wt% (for TMAEMC) V-50, $w_{mon,0}$ = 0.10 and different initial monomer compositions ($f_{MAPTAC,0/TMAEMC,0}$ = 0.1(□), 0.3(Δ), 0.5(×), 0.7(+), 0.9(◊), 1(•)).

It is informative to compare these results to those obtained for TMAEMC copolymerized with AA at identical conditions, although with a lowered V-50 level; the corresponding conversion profiles are shown in Figure 3c, and TMAEMC composition drift in Figure 3d. The influence of TMAEMC content on the conversion rates is minimal for AA-TMAEMC copolymerization, except for the slightly higher rate observed with $f_{TMAEMC,0}$ = 0.10. In contrast, addition of AA at any level significantly increases the rate of monomer conversion for AA-MAPTAC compared to MAPTAC homopolymerization. The azeotropic behavior (i.e., minimal drift in comonomer composition) occurs at a lowered MAPTAC molar fraction (between 0.5 and 0.7) compared to that observed for TMAEMC at $f_{TMAEMC,0}$ = 0.90 as initial monomer concentration was decreased from 10 to 5 wt% [29]. The relative reactivity of

MAPTAC was also reduced from that of TMAEMC when copolymerized with acrylamide [5,34,35], a result consistent with MAPTAC's lowered homopolymerization rate and k_p values (Figure 1), and its copolymerization with AA in this study relative to AA-TMAEMC.

Both the counterion concentration (C_{Cl^-}) and the charge density of the cationic polyelectrolyte formed during polymerization depends on initial MAPTAC molar fraction and total monomer concentration [36]. Thus, AA-MAPTAC copolymerizations were also carried out at $w_{mon,0}$ levels of 0.05, 0.20 and 0.40 to study the combined influence of initial monomer composition and total monomer concentration (both affecting C_{Cl^-}) on rates of polymerization and comonomer composition drifts. The polymerization rates are grouped according to $w_{mon,0}$ in Figure S2 and $f_{MAPTAC,0}$ in Figure 4, which also includes a plot of the comonomer composition drifts for the complete set of experiments. Figure S2 demonstrates that there is a decrease in the polymerization rate with increased MAPTAC fraction at all monomer contents, as seen for $w_{mon,0}$ = 0.10 in Figure 3a. The decrease in polymerization rate with increasing $w_{mon,0}$ from 0.05 to 0.40 is more pronounced as $f_{MAPTAC,0}$ increases from 0.3 (Figure 4a) to 0.9 (Figure 4c), with the relative decrease smaller for all comonomer compositions than observed for MAPTAC homopolymerization [26].

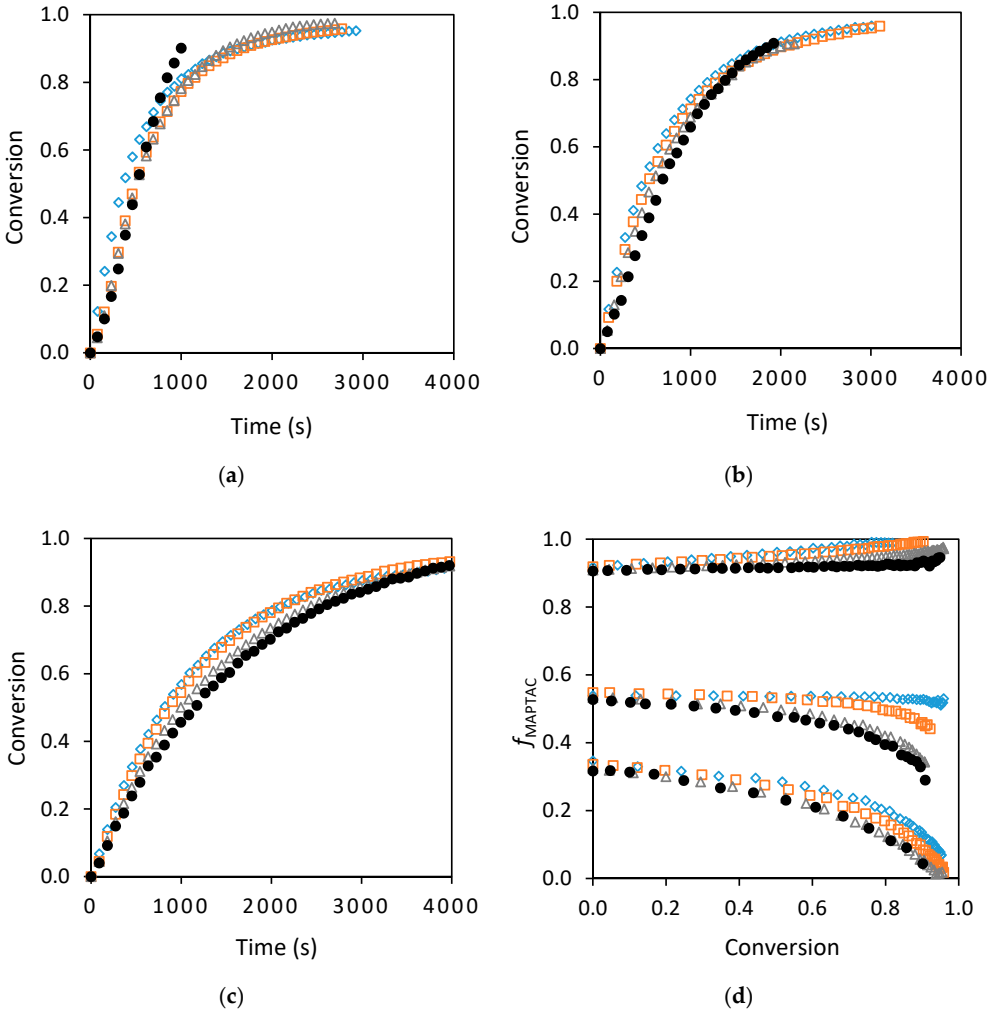

Figure 4. Overall monomer conversion profiles for AA-MAPTAC copolymerization with $f_{MAPTAC,0}$ of (**a**) 0.3 (**b**) 0.5 and (**c**) 0.9 at 50 °C and 0.80 wt% V-50 with varying $w_{mon,0}$ of 0.05(◊), 0.10(□), 0.20(Δ), 0.40(●). The corresponding changes in comonomer composition are shown in (**d**) as a function of overall monomer conversion.

The drift in f_{TMAEMC} for AA-TMAEMC copolymerization was observed to be more pronounced as $w_{mon,0}$ increased from 0.05 to 0.40 [29], and the same is found for the AA-MAPTAC system, as seen for f_{MAPTAC} in Figure 4d. However, the influence of $w_{mon,0}$ is weaker for the MAPTAC copolymerization system, with little difference seen between the curves for $w_{mon,0}$ at 0.20 and 0.40. There is no observable composition drift with $f_{MAPTAC,0}$ = 0.5 and $w_{mon,0}$ = 0.05, indicating that these conditions lead to an azeotropic copolymerization. The difference in azeotropic behavior of MAPTAC (Figure 3b) and TMAEMC (Figure 3d and [29]) is likely related to the lowered k_p of MAPTAC relative to TMAEMC, as well as its lowered sensitivity to C_{Cl^-} (Figure 1), as will be further illustrated in the modeling section of this study.

AA-MAPTAC copolymerizations were also carried out with 1.0 mol·L^{-1} added NaCl and $w_{mon,0}$ of 0.10 at $f_{MAPTAC,0}$ = 0.3, 0.5 and 0.9, to explore how manipulating C_{Cl^-} by addition of NaCl affects copolymerization kinetics. Figure 5a–c demonstrates that there is a consistent slight decrease in conversion rates with added NaCl. As shown in Figure 5d, addition of NaCl increases the relative rate of incorporation of MAPTAC into the copolymer (i.e. lowers f_{MAPTAC} compared to the cases without salt), although to a lesser extent compared to AA-TMAEMC copolymerization [29].

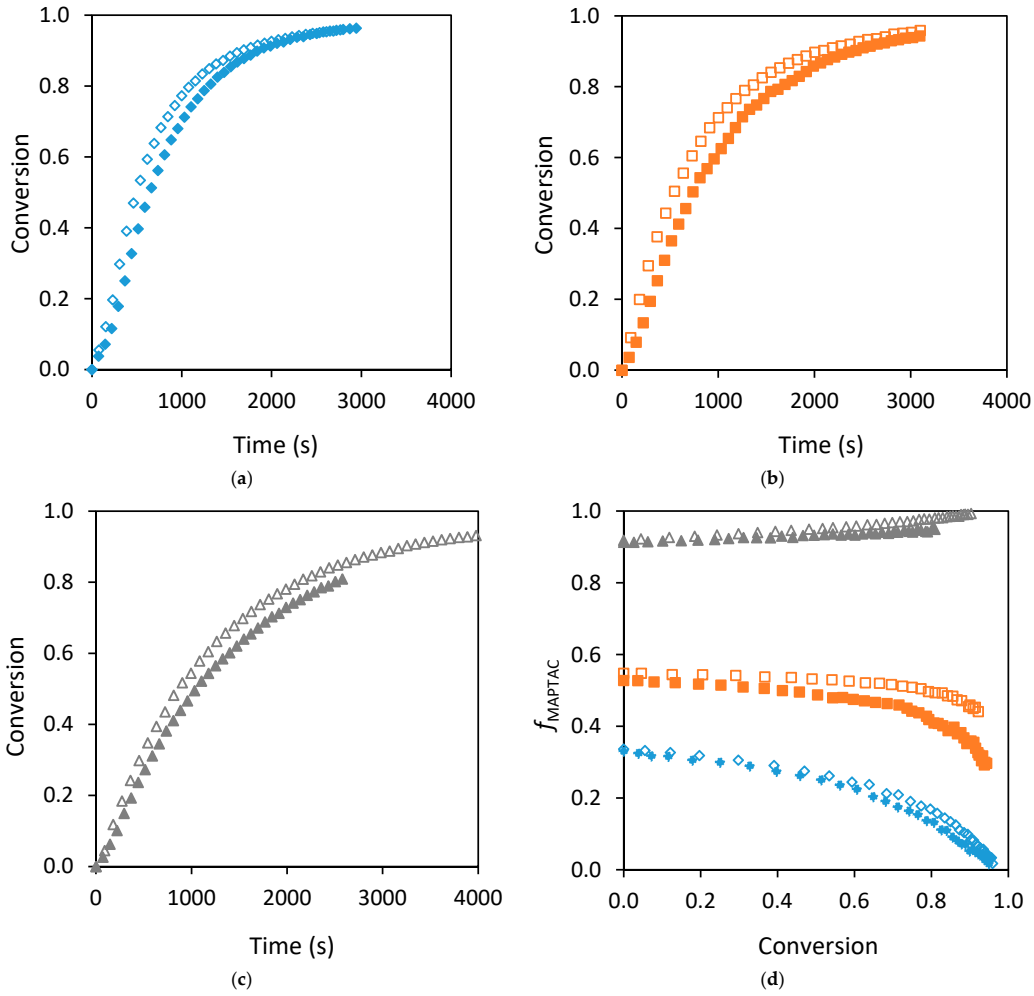

Figure 5. Overall monomer conversion profiles for AA-MAPTAC copolymerization with $f_{MAPTAC,0}$ of (**a**) 0.3 (**b**) 0.5 and (**c**) 0.9 at 50 °C, 0.80 wt% V-50, and $w_{mon.0}$ = 0.10 without NaCl (open symbols) and with 1.0 mol·L^{-1} NaCl (closed symbols). The corresponding comonomer composition drifts are shown in (**d**) as a function of overall monomer conversion.

As shown in Figure S3a, the pH of MAPTAC monomer in aqueous solution is close to 7 and relatively independent of w_{mon}, while the values are below 3 for AA-MAPTAC comonomer mixtures

and decrease with increasing AA content; the pH of the comonomer mixture also decreases with an increase in $w_{mon,0}$, as shown in Figure S3b. This suggests that polymerization rate is controlled by the influence of C_{Cl^-} on MAPTAC reactivity, as the AA remains in nonionized form under all reaction conditions; the same conclusion was reached for the AA-TMAEMC system [29]. To further study the specific influence of AA on kinetics, conversion profiles were compared for experiments that substituted propionic acid (PA) as a non-reactive version of AA while maintaining the total MAPTAC and acid weight fraction at 0.10; the copolymerization of MAPTAC with AA at $f_{AA,0}$ = 0.7 and 0.5 was compared to MAPTAC homopolymerization with PA molar fraction of 0.7 and 0.5 (replacing AA monomer), and also MAPTAC homopolymerization at the natural pH. The faster reaction rate of the copolymerization reaction relative to the homopolymerization cases (with and without PA) shown in Figure S4 highlights that it is the relative reactivity of the comonomer that influences copolymerization rate under the nonionized conditions of AA, not the decreased pH of the solution.

4. Model Development

With a better understanding of the influence of the reaction environment on kinetics, the approach to represent the copolymerization behavior of cationic monomers can be generalized. To this end, the modeling framework previously implemented in the mechanistic modeling package Predici® (version 11) for TMAEMC homopolymerization [27,37] and AA-TMAEMC copolymerization [29] is used here for the MAPTAC systems, with adjustments to account for weaker influence of counterion concentration on the kinetic rate coefficients. The mechanisms included are initiation, propagation (terminal model for copolymerization), termination (geometric mean for copolymer cross-termination), transfer to monomer and reactions associated with AA backbiting, as summarized in Table 1. The influence of C_{Cl^-} on MAPTAC propagation and termination rate coefficients are established using a combination of the current experimental results and k_p values obtained from PLP-SEC studies [26]. Other treatments of rate coefficients are the same as implemented for MAPTAC and AA [16] homopolymerization models, as summarized in Table 2. The value of the AA homotermination rate coefficient is expressed as a function of the initial monomer/solvent viscosity. Viscosity measurements of AA-MAPTAC mixtures carried out at the same overall monomer contents ($w_{mon,0}$ = 0.025, 0.05 and 0.10) were constant over the range of comonomer compositions (Figure S5). Thus, there was no need to adjust the treatment of the AA k_t value to account for the effect of MAPTAC on solution viscosity of the comonomer mixture in water. As also seen in the studies on TMAEMC homopolymerization and AA-TMAEMC copolymerization, the viscosity of *p*MAPTAC solution is significantly higher than that of the monomer solutions (Figure S6); although the viscosity of the systems increases substantially during polymerization, the increase does not influence termination kinetics which are dominated by electrostatic interactions [27,29].

Table 1. Reaction steps included in the AA-MAPTAC copolymerization model.

Initiation
$I \xrightarrow{k_i} 2fI^*$
$I^* + MAPTAC \xrightarrow{k_p^{MAPTAC}} P_1^{MAPTAC}$; $I^* + AA \xrightarrow{k_p^{AA}} P_1^{AA}$
Chain Propagation
$P_n^{MAPTAC} + MAPTAC \xrightarrow{k_p^{MAPTAC}} P_{n+1}^{MAPTAC}$
$P_n^{AA} + AA \xrightarrow{k_p^{AA}} P_{n+1}^{AA}$
$P_n^{MAPTAC} + AA \xrightarrow{k_p^{MAPTAC\cdot AA}} P_{n+1}^{AA}$
$P_n^{AA} + MAPTAC \xrightarrow{k_p^{AA\cdot MAPTAC}} P_{n+1}^{MAPTAC}$

Table 1. *Cont.*

Transfer to Monomer
$P_n^{MAPTAC} + MAPTAC \xrightarrow{k_{tr}^{MAPTAC}} D_n + P_1^{MAPTAC}$
$P_n^{AA} + AA \xrightarrow{k_{tr}^{AA}} D_n + P_1^{AA}$
$P_n^{AA} + MAPTAC \xrightarrow{k_{tr}^{AA\cdot MAPTAC}} D_n + P_1^{MAPTAC}$
$P_n^{MAPTAC} + AA \xrightarrow{k_{tr}^{MAPTAC\cdot AA}} D_n + P_1^{AA}$
Termination SPR-SPR
$P_n^{MAPTAC} + P_m^{MAPTAC} \xrightarrow{(1-\alpha_{ss}^{MAPTAC})k_{t,ss}^{MAPTAC}} D_{n+m} \Big/ \xrightarrow{\alpha_{ss}^{MAPTAC}k_{t,ss}^{MAPTAC}} D_n + D_m$
$P_n^{AA} + P_m^{AA} \xrightarrow{(1-\alpha_{ss}^{AA})k_{t,ss}^{AA}} D_{n+m} \Big/ \xrightarrow{\alpha_{ss}^{AA}k_{t,ss}^{AA}} D_n + D_m$
$P_n^{AA} + P_m^{MAPTAC} \xrightarrow{(1-\alpha_{ss}^{AA\cdot MAPTAC})k_{t,ss}^{AA\cdot MAPTAC}} D_{n+m} \Big/ \xrightarrow{\alpha_{ss}^{AA\cdot MAPTAC}k_{t,ss}^{AA\cdot MAPTAC}} D_n + D_m$
Reactions Related to Backbiting
Backbiting
$P_n^{AA} \xrightarrow{F_{AA}k_{bb}} Q_n^{AA}$
Addition to MCR
$Q_n^{AA} + AA \xrightarrow{k_{p,tert}^{AA\cdot AA}} P_{n+1}^{AA}$
$Q_n^{AA} + MAPTAC \xrightarrow{k_{p,tert}^{AA\cdot MAPTAC}} P_{n+1}^{MAPTAC}$
Cross Termination MCR-SPR
$P_n^{MAPTAC} + Q_m^{AA} \xrightarrow{(1-\alpha_{st}^{MAPTAC\cdot AA})k_{t,st}^{MAPTAC\cdot AA}} D_{n+m} \Big/ \xrightarrow{\alpha_{st}^{MAPTAC\cdot AA}k_{t,st}^{MAPTAC\cdot AA}} D_n + D_m$
$P_n^{AA} + Q_m^{AA} \xrightarrow{(1-\alpha_{st}^{AA\cdot AA})k_{t,st}^{AA\cdot AA}} D_{n+m} \Big/ \xrightarrow{\alpha_{st}^{AA\cdot AA}k_{t,st}^{AA\cdot AA}} D_n + D_m$
Termination MCR-MCR
$Q_n^{AA} + Q_m^{AA} \xrightarrow{(1-\alpha_{tt}^{AA})k_{t,tt}^{AA}} D_{n+m} \Big/ \xrightarrow{\alpha_{tt}^{AA}k_{t,tt}^{AA}} D_n + D_m$

* Termination occurs by combination to yield product chains of length $n + m$, or by disproportionation. α and $(1 - \alpha)$ represent the fraction of termination by disproportionation and combination respectively, with subscripts introduced for secondary propagating radicals (s) and midchain radicals (t).

Table 2. Rate coefficients and expressions used in AA-MAPTAC copolymerization model.

Rate Expression	Reference
Initiation	
$k_d\left(s^{-1}\right) = 9.24 \times 10^{14} \exp\left(-\frac{124}{RT}\ \frac{kJ}{mol}\right)$ $f = 0.8$	[38]
Chain propagation	
$k_p^{MAPTAC}\left(\frac{L}{mol.s}\right) = k_{p,0}^{MAPTAC}(1.0 + 0.5C_{Cl^-})$ $k_{p,0}^{MAPTAC}\left(\frac{L}{mol.s}\right) = 4.23{\cdot}10^5 \exp\left(-\frac{1924}{T}K\right)$	[26]
$k_p^{AA}\left(\frac{L}{mol.s}\right) = k_{p0}^{AA}(0.11 + (1 - 0.11)\ \exp(-3.0w_m\prime))$ $k_{p0}^{AA}\left(\frac{L}{mol.s}\right) = 3.2{\cdot}10^7 \exp\left(-\frac{1564}{T}\right)$	[16]
$r_{AA} = 0.36$, $r_{MAPTAC} = a(1.0 + C_{Cl^-})$ where $a = 0.46$	this work
$k_P^{MAPTAC.AA}\left(\frac{L}{mol.s}\right) = \frac{k_{p,0}^{MAPTAC}}{0.46}$; $k_P^{AA.MAPTAC}\left(\frac{L}{mol.s}\right) = \frac{k_P^{AA}}{0.36}$	this work

Table 2. *Cont.*

Rate Expression	Reference
Transfer/Cross-transfer to Monomer	
$k_{tr}^{MAPTAC}\left(\frac{L}{mol.s}\right) = 2.89{\cdot}10^{-6}$	This work
$k_{tr}^{AA}\left(\frac{L}{mol.s}\right) = 7.5{\cdot}10^{-5}k_p^{AA}$	[16]
$k_{tr}^{AA{\cdot}MAPTAC}\left(\frac{L}{mol.s}\right) = k_{tr}^{MAPTAC}\frac{k_p^{AA}}{r_{AA}{\cdot}k_p^{MAPTAC}}$	This work
$k_{tr}^{MAPTAC{\cdot}AA}\left(\frac{L}{mol.s}\right) = k_{tr}^{AA}\frac{k_p^{MAPTAC}}{r_{MAPTAC}{\cdot}k_p^{AA}}$ $= C_{tr}^{AA}\frac{k_{p,0}^{MAPTAC}}{r_{MAPTAC}}$	This work
Termination SPR-SPR:	
$k_{t,ss}^{MAPTAC}(1,1)\left(\frac{L}{mol{\cdot}s}\right) = 4.8{\cdot}10^{8}\exp\left(-\frac{998}{T}K\right)(0.19 + 1.37C_{Cl^-})$	
where $\alpha_s = 0.62$; $\alpha_1 = 0.18$; $i_c = 45$	[27,39]
$k_{t,ss}^{AA}(1,1)\left(\frac{L}{mol{\cdot}s}\right) = 9.78{\cdot}10^{11}\exp\left(-\frac{1858}{T}K\right)viscosity_{corr}$	[39,40]
$viscosity_{corr} = 1.56 - 1.77w_{mon,o} - 1.2{w_{mon,o}}^2 + 2.43{w_{mon,o}}^3$	[16]
where $\alpha_s = 0.6$; $\alpha_1 = 0.16$; $i_c = 30$	[16]
$\langle k_{t,ss}^{AA.MAPTAC}\rangle\left(\frac{L}{mol{\cdot}s}\right) = \Phi{\cdot}\left(\langle k_{t,ss}^{AA}\rangle{\cdot}\langle k_{t,ss}^{MAPTAC}\rangle\right)^{1/2}$	This work
$\alpha_{ss}^{MAPTAC} = 0.8$; $\alpha_{ss}^{AA} = 0.05$; $\alpha_{ss}^{AA.MAPTAC} = 0.4$	[16,39]
Backbiting	
$k_{bb}^{AA}\left(s^{-1}\right) = F_{AA}^{inst}9.94{\cdot}10^{8}\exp\left(-\frac{4576}{T}K\right)$	[16]
Addition to MCR	
$k_{p,tert}^{AA}\left(\frac{L}{mol{\cdot}s}\right) = 0.755\ \exp\left(-\frac{2464}{T}K\right)k_p^{AA}$	[16]
Cross Termination MCR-SPR	
$\langle k_{t,st}^{AA.AA}\rangle\left(\frac{L}{mol{\cdot}s}\right) = 0.3\ \langle k_{t,ss}^{AA}\rangle$	[16,23]
$\langle k_{t,st}^{MAPTAC.AA}\rangle\left(\frac{L}{mol{\cdot}s}\right) = 0.3\ \langle k_{t,ss}^{AA.MAPTAC}\rangle$	This work
$\alpha_{st}^{MAPTAC.AA} = 0.8$; $\alpha_{st}^{AA.AA} = 0.4$	This work, [16]
Termination MCR-MCR	
$\langle k_{t,st}^{MAPTAC.AA}\rangle\left(\frac{L}{mol{\cdot}s}\right) = 0.3\ \langle k_{t,ss}^{AA.MAPTAC}\rangle$ $\alpha_{tt}^{AA} = 0.8$	[16,23]
Density	
$\rho_{AA}\left(g{\cdot}mL^{-1}\right) = 1.0731 - 1.0826\times10^{-3}T\left(^{\circ}C^{-1}\right) - 7.2379\times10^{-7}T\left(^{\circ}C^{-2}\right)$	[16]
$\rho_{H2O}\left(g{\cdot}mL^{-1}\right) = 0.9999 - 2.3109\times10^{-5}T\left(^{\circ}C^{-1}\right) - 5.4481\times10^{-6}T\left(^{\circ}C^{-2}\right)$	[16]
$\rho_{MAPTAC}\left(g{\cdot}mL^{-1}\right) = 0.9806 - 4.5523\times10^{-4}T\left(^{\circ}C^{-1}\right) + 1.1040\times10^{-7}T\left(^{\circ}C^{-2}\right)$	[26]

w_m' refers to AA + MAPTAC monomer content on a polymer free basis.

The systematic decrease of rate of conversion (and thus $k_p/<k_t>^{0.5}$) observed with increased MAPTAC content [26], also observed in TMAEMC homopolymerization [27], implies that $<k_t>$ increases more strongly with C_{Cl^-} in the system than k_p. As there are no independent studies of MAPTAC termination kinetics, it is assumed that k_t^{MAPTAC} follows the same functional form as used to represent k_t^{TMAEMC}, both in terms of temperature and chain-length dependencies [27,39] as well as the dependence on C_{Cl^-}. The parameters for the latter relationship were determined by fitting the conversion profiles of the MAPTAC homopolymerizations measured at 50 °C [26] to the empirical relation $k_t(1,1) = a + bC_{Cl^-} + cC_{Cl^-}^2$ using the parameter estimation capabilities of Predici. As shown in

Figure 6, and in contrast to the TMAEMC homopolymerization system, the increase in $k_t(1,1)$ values is linear with total C_{Cl}^- in solution. The best-fit values obtained for the $k_t(1,1)$ parameters are 0.19 ± 0.04, 1.37 ± 0.13, and 0.002 ± 0.08 for *a*, *b* and *c*, respectively; thus, the quadratic term was not used in the $k_t(1,1)$ representation. These values indicate a higher termination of charged MAPTAC macroradicals at lower monomer contents compared to TMAEMC up to $w_{mon,0}$ of 0.20 with the opposite observed at higher monomer contents. Figure 7 shows that the representation of the MAPTAC homopolymerization conversion profiles obtained for $w_{mon,0}$ between 0.05 and 0.35 at 50 °C with 0.80 wt% V-50 is excellent over the full range of polymerizations.

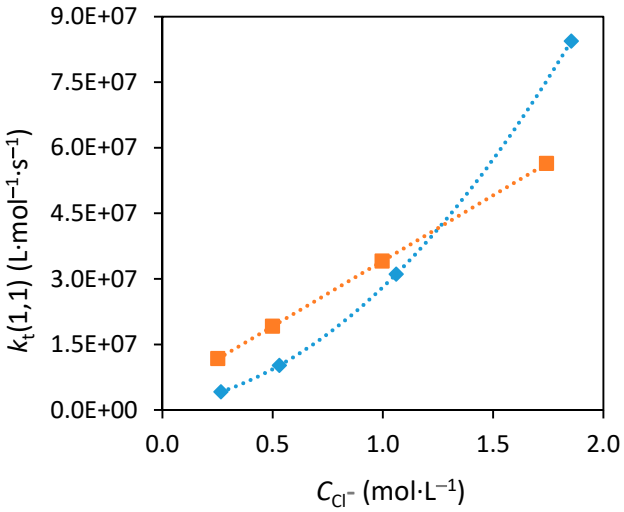

Figure 6. Estimated variation of $k_t(1,1)$ as a function of counterion concentration from fits to TMAEMC (♦) [27] and MAPTAC (■) [26] homopolymerizations carried out at 50 °C and varying initial monomer content in aqueous solution.

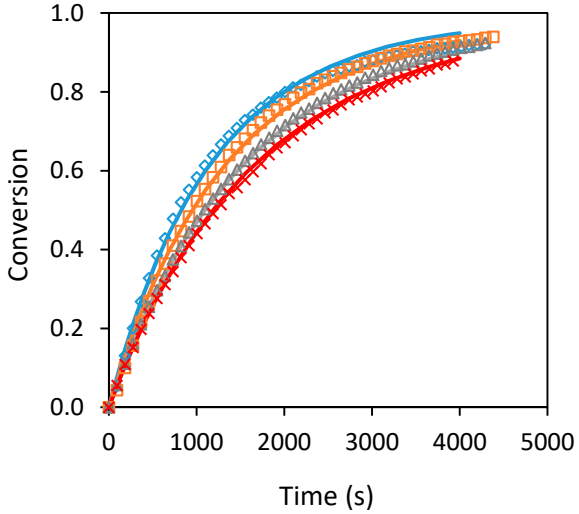

Figure 7. Comparison of experimental (symbol) and simulated (lines) batch conversion profiles collected at varying $w_{mon,0}$ of 0.05 (◊), 0.10 (□), 0.20 (Δ) and 0.35 (×) at 50 °C with 0.80 wt% V-50 in aqueous solution. Experimental results taken from [26], with simulations generated using the model summarized in Tables 1 and 2.

The rate coefficients used to represent AA [16] and MAPTAC homopolymerization are combined for the representation of AA-MAPTAC copolymerization following the approach used to develop the model of AA-TMAEMC copolymerization [29]. The model includes the backbiting mechanisms that result from presence of AA monomer and radicals in the copolymerization system. The previous study

by Wittenberg et al. [16] provides the rate coefficients for AA backbiting and the subsequent reactions involving the midchain radicals. Parameter estimation in Predici is used to estimate k_t^{cross} from the copolymer conversion profiles after first fitting the comonomer composition drifts to determine the system reactivity ratios.

4.1. Estimation of Reactivity Ratios from Comonomer Composition Drifts

As the pH of the system indicates that AA does not ionize under polymerization conditions, it can be assumed that only the addition of MAPTAC to a radical with a MAPTAC terminal unit is influenced by electrostatic effects. Thus, r_{AA} is assumed to be constant, while r_{MAPTAC} varies with C_{Cl^-} following the same functional form as k_p^{MAPTAC}:

$$r_{MAPTAC} = a \cdot (1 + 0.5\, C_{Cl^-}) \tag{1}$$

The experimental comonomer composition drifts obtained over a range of $w_{mon,0}$ and $f_{MAPTAC,0}$ levels (Figures 3b and 4d) are used to estimate reactivity ratios assuming terminal model kinetics, with the instantaneous copolymer composition given by:

$$F_{MAPTAC} = \frac{r_{MAPTAC} f_{MAPTAC}^2 + f_{MAPTAC} f_{AA}}{r_{MAPTAC} f_{MAPTAC}^2 + 2 f_{MAPTAC} f_{AA} + r_{AA} f_{AA}^2} \tag{2}$$

The molar fraction of MAPTAC in the comonomer mixture is $f_{MAPTAC} = [MAPTAC]/([MAPTAC] + [AA])$, and reactivity ratios are defined by $r_{MAPTAC} = k_p^{MAPTAC}/k_p^{MAPTAC.AA}$ and $r_{AA} = k_p^{AA}/k_p^{AA.MAPTAC}$. These parameters were estimated by the model to fit the change in comonomer composition with conversion using the direct numerical integration (DNI) method [41]:

$$\frac{df_{MAPTAC}}{dx} = \frac{f_{MAPTAC} - F_{MAPTAC}}{1 - x} \tag{3}$$

with initial condition $f_{MAPTAC} = f_{MAPTAC,0}$ at $x = 0$. This technique has been previously used for the estimation of reactivity ratios for copolymerization of AA with both non-ionized AM [42] and cationic TMAEMC [29] monomers from experimental results obtained by the in situ NMR technique across a wide range of initial conditions. The only additional modification for charged systems is to express the reactivity ratio of the cationic component as a function of monomer content according to Equation (1). Estimation using the experimental results shown in Figures 3b and 4d results in estimated values of $r_{AA} = 0.36 \pm 0.006$ and $a = 0.46 \pm 0.006$, with the fit compared to the experimental data in Figure 8. The faster relative incorporation of MAPTAC into the copolymer at higher $w_{mon,0}$ (and thus C_{Cl^-}) is well captured by the model. Furthermore, excellent representations are obtained (without additional fitting) for the increased relative consumption of MAPTAC with added NaCl (Figure 8c) as well as the azeotropic behavior beyond $f_{MAPTAC,0} = 0.5$. Therefore, the effects of initial monomer concentration and added NaCl on the MAPTAC composition drifts are accurately captured using the same functional representation that was developed for AA-TMAEMC copolymerization.

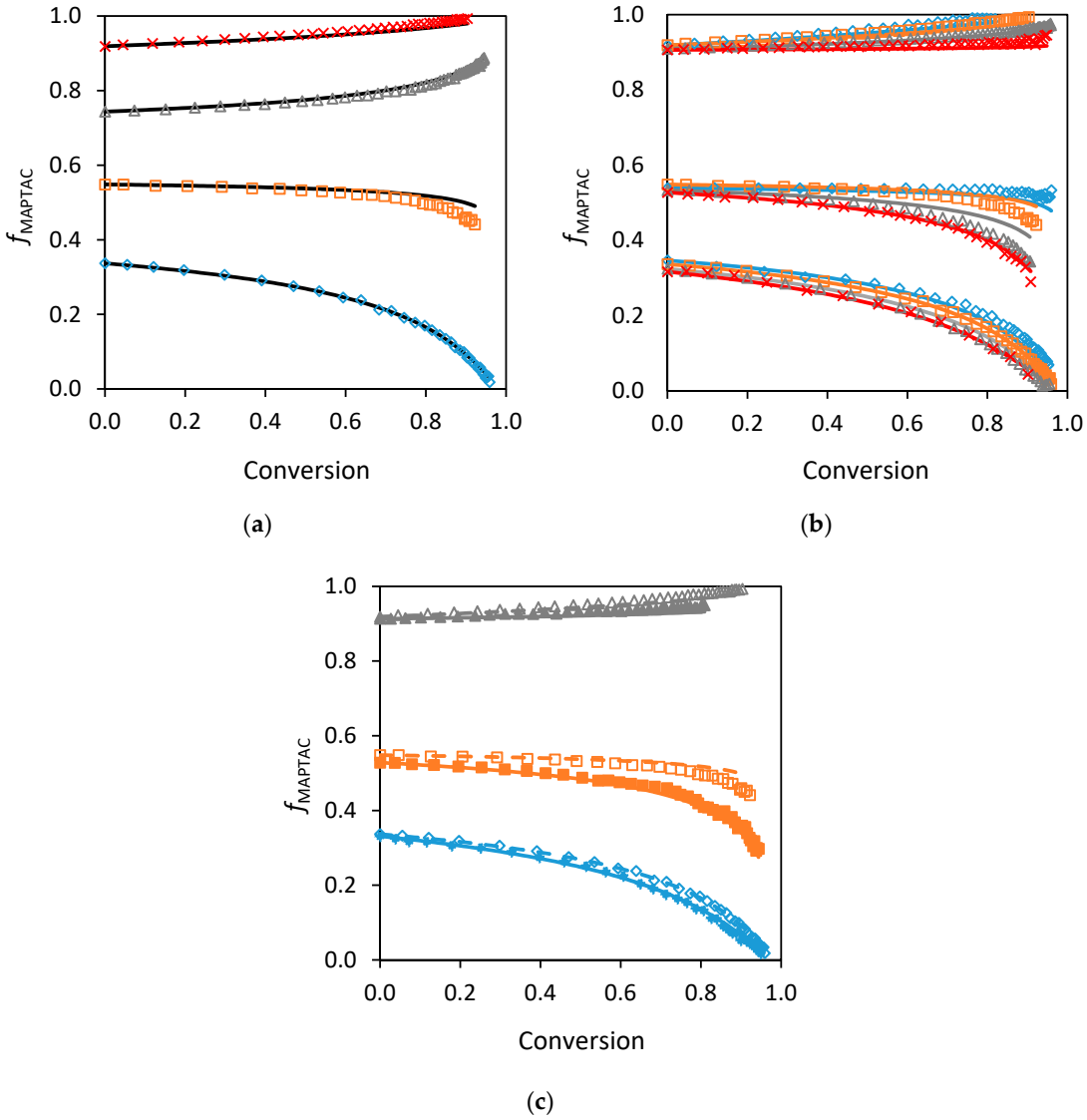

Figure 8. Comparison of batch comonomer composition drifts for AA-MAPTAC copolymerizations at 50 °C and 0.80 wt% V-50 at different initial monomer compositions with (**a**) $w_{mon,0}$ = 0.10; (**b**) $w_{mon,0}$ = 0.05(◊), 0.10(□), 0.20(Δ) and 0.40(×) at different initial monomer compositions; and (**c**) for $w_{mon,0}$ = 0.10 without (open symbols) and with 1.0 mol·L^{-1} NaCl (closed symbols). Lines are model representations of the composition drift developed using Equations (1)–(3), with parameters summarized in Table 2.

4.2. Model Fit of Conversion Profiles

Using the Predici software, the set of reaction mechanisms and rate coefficients listed in Tables 1 and 2 are combined with the expressions and values obtained for reactivity ratio estimations to develop a full kinetic model to simulate the conversion profiles obtained experimentally using the assumptions made to model AA-TMAEMC copolymerization [29]. It is informative to examine the terminal model propagation kinetics that leads to the following expression for the composition-averaged k_p^{cop}:

$$k_p^{cop} = \frac{r_{MAPTAC} f_{MAPTAC}^2 + 2 f_{MAPTAC} f_{AA} + r_{AA} f_{AA}^2}{r_{MAPTAC} f_{MAPTAC} / k_p^{MAPTAC} + r_{AA} f_{AA} / k_p^{AA}} \quad (4)$$

k_p^{MAPTAC} is two orders of magnitude lower than k_p^{AA}, and thus controls the averaged rate coefficient, as shown by the plot of log k_p^{cop} against f_{MAPTAC} in Figure 9. The k_p^{cop} values for MAPTAC gradually

decrease as f_{MAPTAC} increases in the system, consistent with experimental results and in contrast to the sharper decrease seen upon addition of TMAEMC to AA, with little change between $f_{TMAEMC,0}$ of 0.1 and 1.0. Also, the terminal model treatment captures the lower influence of C_{Cl^-} in MAPTAC compared to TMAEMC as seen in the smaller difference in the curves generated with w_{mon} of 0.10 and 0.40.

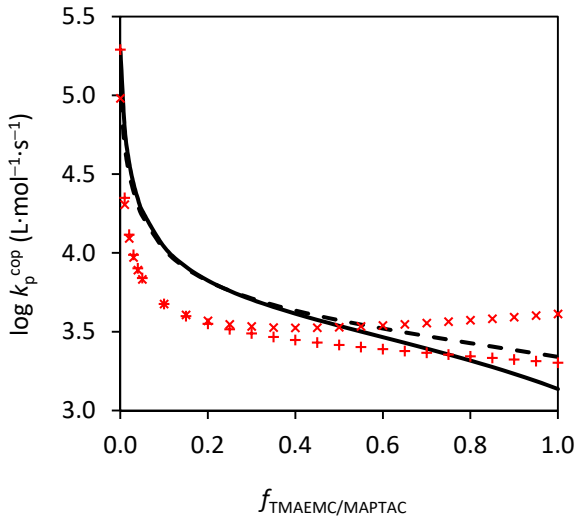

Figure 9. Comparison of log k_p^{cop} calculated at 50 °C as a function of MAPTAC/TMAEMC molar fraction at $w_{mon,0}$ = 0.10 (—) and 0.40 (- - -) for MAPTAC and $w_{mon,0}$ = 0.10 (+) and 0.40 (×) for TMAEMC.

Various approaches to represent cross-termination of the TMAEMC and AA copolymerization system were investigated in the previous investigation [29], an important task due to the more than two order of magnitude difference between the termination rate coefficients for homopolymerization of AA and that of the charged cationic (either TMAEMC or MAPTAC) system. The best representation of the AA-TMAEMC conversion profiles was obtained using the geometric mean treatment [29], an assumption also used here to model AA-MAPTAC copolymerization:

$$\langle k_{t,ss}^{AA.MAPTAC} \rangle = \Phi \cdot \left(\langle k_{t,ss}^{AA} \rangle \cdot \langle k_t^{MAPTAC} \rangle \right)^{1/2} \quad (5)$$

The complete set of copolymerization experiments run across different conditions (monomer concentration and composition) were used to perform parameter estimation of the single fitting parameter, with the best fit Φ value of 2.9 ± 0.2 obtained. The resulting representation of the conversion profiles is shown in Figure 10 grouped according to $w_{mon,0}$. Except for slight underpredictions of conversion rates for $w_{mon,0}$ = 0.05 (Figure 10a, $f_{MAPTAC,0}$ = 0.3 and 0.5), the effects of both $w_{mon,0}$ and $f_{MAPTAC,0}$ on conversion rates are well captured by the model. A similar underprediction of conversion rates at low $f_{TMAEMC,0}$ and low monomer concentrations was found in the AA-TMAEMC copolymerization study and was attributed to overprediction of the influence of AA backbiting on rate [29]. Despite this minor issue, the model, using the same assumptions and functional forms as developed for AA-TMAEMC, is able to describe the AA-MAPTAC copolymerization system over a wide range of monomer contents and the complete range of comonomer compositions, including MAPTAC homopolymerization (Figure 7).

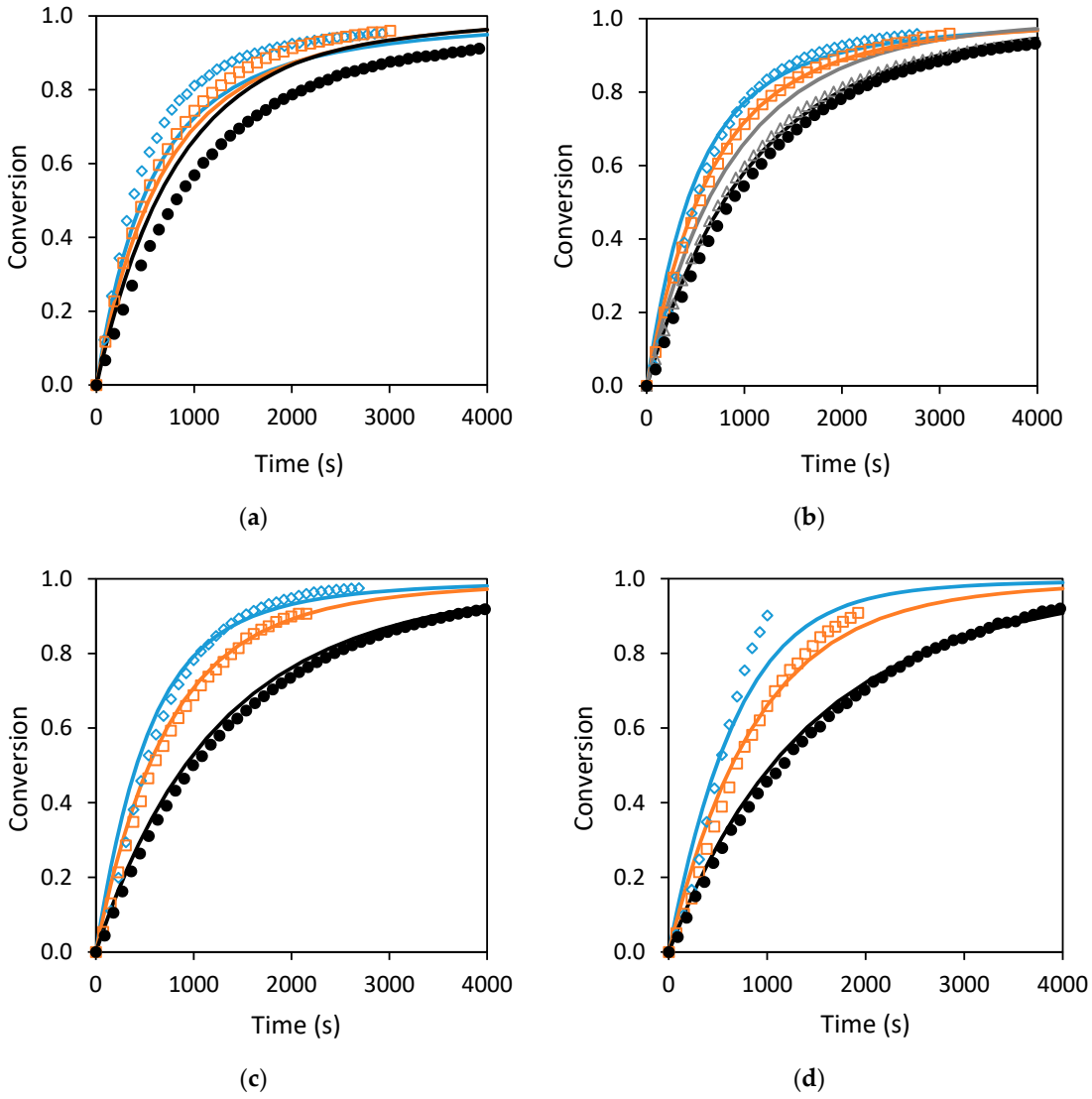

Figure 10. Simulated conversion profiles (lines) compared to experimental results (points) for $f_{MAPTAC,0}$ = 0.3(◊), 0.5(□), 0.7(Δ) and 0.9(●) at 50 °C and 0.80 wt% V-50 with $w_{mon,0}$ of (**a**) 0.05, (**b**) 0.10, (**c**) 0.20 and (**d**) 0.40. Profiles are calculated using the model summarized in Tables 1 and 2, with the copolymer termination rate coefficient calculated using the geometric mean method (best fit Φ values = 2.9).

5. Conclusions

An extensive investigation of the synthesis of polyelectrolytes from the aqueous-phase copolymerization of the cationic monomer MAPTAC with nonionized AA was conducted, to broaden and generalize the knowledge of copolymerization kinetics of cationic monomers. The rates of polymerization and relative consumption rates of AA and MAPTAC as a function of conversion were measured across varying initial monomer contents ($w_{mon,0}$ = 0.05 − 0.35) and initial comonomer compositions, with some experiments conducted with added salt to manipulate counterion concentration. Functional representations of MAPTAC propagation and termination rate coefficients were formulated to capture the effect of charge screening on the rate coefficients, extended to also represent the influence of C_{Cl^-} on comonomer composition drifts. As found for the TMAEMC system, an increase in $w_{mon,0}$ resulted in increased relative incorporation of MAPTAC into the copolymer, indicative of reduced electrostatic repulsion. The correctness of this interpretation is verified by the ability of the representation to also capture the influence of adding NaCl on the comonomer

composition drift. Compared to TMAEMC, the influence of C_{Cl^-} on MAPTAC copolymer composition was not as strong, in agreement to the PLP-SEC study of homopropagation kinetics.

A comparison to the AA-TMAEMC system demonstrates that the same generalized model structure can be used to represent copolymerizations of AA with both cationic monomers, despite the amide vs ester functionality. The terminal model of propagation was combined with a treatment of AA intramolecular chain transfer to develop a complete mechanistic representation of AA-MAPTAC copolymerization. Monomer conversions profiles were well represented by combining homopolymerization models combined with the geometric mean treatment of cross-termination. However, further experiments are required to test the ability of the model to represent conversion and copolymer composition profiles, as well as copolymer molecular weights, over a range of operating temperature.

Supplementary Materials: Additional results documenting experimental reproducibility (Figure S1), solution pH (Figure S3), additional copolymerization conversion profiles (Figures S2 and S4) and solution viscosity (Figures S5 and S6) are available online at http://www.mdpi.com/2227-9717/8/11/1352/s1.

Author Contributions: Conceptualization, experimentation, analysis, draft preparation, I.H.E.; experimentation, E.S.; supervision, project administration, funding acquisition, writing review and editing, R.A.H. All authors have read and agreed to the published version of the manuscript.

Funding: This research was funded by BASF SE, Ludwigshafen, Germany.

Acknowledgments: The authors are grateful to BASF SE for financial support. Also, the technical discussions with Hugo Vale (BASF) and Igor Lacík (Polymer Institute of the Slovak Academy of Sciences) are appreciated.

Conflicts of Interest: The authors declare no conflict of interest.

References

1. Wesley, L.; Whippie, H.Z. Water-soluble free radical addition polymerizations. In *Monitoring Polymerization Reactions: From Fundamentals to Applications*; Alb, A.M., Reed, W.F., Eds.; Wiley-Interscience: Hoboken, NJ, USA, 2014.
2. Mandel, M. Polyelectrolytes. In *Encyclopedia of Polymer Science and Engineering*, 2nd ed.; Mark, H.F., Bikales, N., Overberger, C.G., Menges, G., Eds.; Wiley: New York, NY, USA, 1988; Volume 11, p. 739.
3. Heitner, N. Flocculating agents. In *Kirk-Othmer Encyclopedia of Chemical Technology*; Kroschwitz, J.I., Howe-Grant, M., Eds.; Wiley: New York, NY, USA, 2004; Volume 11.
4. BASF Home Page. Available online: http://www.basf.com/global/en.html (accessed on 12 February 2019).
5. Nicke, R. Flocculating agents help to increase the production. *Zellst. Und Pap.* **1982**, *31*, 19–23.
6. Beuermann, S.; Buback, M. Rate coefficients of free-radical polymerization deduced from pulsed laser experiments. *Prog. Polym. Sci.* **2002**, *27*, 191–254. [CrossRef]
7. Buback, M.; Schroeder, H.; Kattner, H. Detailed kinetic and mechanistic insight into radical polymerization by spectroscopic techniques. *Macromolecules* **2016**, *49*, 3193–3213. [CrossRef]
8. Beuermann, S.; Buback, M.; Hesse, P.; Lacík, I. Free-radical propagation rate coefficient of nonionized methacrylic acid in aqueous solution from low monomer concentrations to bulk polymerization. *Macromolecules* **2006**, *39*, 184–193. [CrossRef]
9. Beuermann, S.; Buback, M.; Hesse, P.; Kutcha, F.-D.; Lacík, I.; Van Herk, A.M. Critically evaluated rate coefficients for free-radical polymerization Part 6: Propagation rate coefficient of methacrylic acid in aqueous solution (IUPAC Technical Report). *Pure Appl. Chem.* **2007**, *79*, 1463–1469. [CrossRef]
10. Lacík, I.; Učňová, L.; Kukučková, S.; Buback, M.; Hesse, P.; Beuermann, S. Propagation rate coefficient of free-radical polymerization of partially and fully ionized methacrylic acid in aqueous solution. *Macromolecules* **2009**, *42*, 7753–7761. [CrossRef]
11. Beuermann, S.; Buback, M.; Hesse, P.; Hutchinson, R.A.; Kukučková, S.; Lacík, I. Termination kinetics of the free-radical polymerization of nonionized methacrylic acid in aqueous solution. *Macromolecules* **2008**, *41*, 3513–3520. [CrossRef]
12. Lacík, I.; Beuermann, S.; Buback, M. PLP−SEC study into free-radical propagation rate of nonionized acrylic acid in aqueous solution. *Macromolecules* **2003**, *25*, 9355–9363. [CrossRef]

13. Lacík, I.; Beuermann, S.; Buback, M. PLP-SEC study into the free-radical propagation rate coefficients of partially and fully ionized acrylic acid in aqueous solution. *Macromol. Chem. Phys.* **2004**, *205*, 1080–1087. [CrossRef]
14. Lacík, I.; Beuermann, S.; Buback, M. Aqueous phase size-exclusion-chromatography used for PLP–SEC studies into free-radical propagation rate of acrylic acid in aqueous solution. *Macromolecules* **2001**, *34*, 6224–6228. [CrossRef]
15. Barth, J.; Meiser, W.; Buback, M. SP-PLP-EPR study into termination and transfer kinetics of non-ionized acrylic acid polymerized in aqueous solution. *Macromolecules* **2012**, *45*, 1339–1345. [CrossRef]
16. Wittenberg, N.F.G.; Preusser, C.; Kattner, H.; Stach, M.; Lacík, I.; Hutchinson, R.A.; Buback, M. Modeling acrylic acid radical polymerization in aqueous solution. *Macromol. React. Eng.* **2016**, *10*, 95–107. [CrossRef]
17. Buback, M.; Hesse, P.; Hutchinson, R.A.; Kasák, P.; Lacík, I.; Stach, M.; Utz, I. Kinetics and modeling of free-radical batch polymerization of nonionized methacrylic acid in aqueous solution. *Ind. Eng. Chem. Res.* **2008**, *47*, 8197–8204. [CrossRef]
18. Wittenberg, N.F.G.; Buback, M.; Hutchinson, R.A. Kinetics and modeling of methacrylic acid radical polymerization in aqueous solution. *Macromol. React. Eng.* **2013**, *7*, 267–276. [CrossRef]
19. Barth, J.; Buback, M. Termination and transfer kinetics of sodium acrylate polymerization in aqueous solution. *Macromolecules* **2012**, *45*, 4152–4157. [CrossRef]
20. Kattner, H.; Drawe, P.; Buback, M. Chain-length-dependent termination of sodium methacrylate polymerization in aqueous solution studied by SP-PLP-EPR. *Macromolecules* **2017**, *50*, 1386–1393. [CrossRef]
21. Drawe, P.; Buback, M.; Lacík, I. Radical polymerization of alkali acrylates in aqueous solution. *Macromol. Chem. Phys.* **2015**, *216*, 1333–1340. [CrossRef]
22. Preusser, C.; Ezenwajiaku, I.H.; Hutchinson, R.A. The combined influence of monomer concentration and ionization on acrylamide/acrylic acid composition in aqueous solution radical batch copolymerization. *Macromolecules* **2016**, *49*, 4746–4756. [CrossRef]
23. Preusser, C. Kinetics and Modeling of Free-Radical Aqueous Phase Polymerization of Acrylamide with Acrylic Acid at Varying Degrees of Ionization. Ph.D. Thesis, Queen's University, Kingston, ON, Canada, August 2015.
24. Riahinezhad, M.; Mcmanus, N.; Penlidis, A. Effect of monomer concentration and ph on reaction kinetics and copolymer microstructure of acrylamide/acrylic acid copolymer. *Macromol. React. Eng.* **2015**, *9*, 100–113. [CrossRef]
25. Riahinezhad, M.; Kazemi, N.; McManus, N.; Penlidis, A. Effect of ionic strength on the reactivity ratios of acrylamide/acrylic acid (sodium acrylate) copolymerization. *J. Appl. Polym. Sci.* **2014**, *131*. [CrossRef]
26. Chovancová, A.; Ezenwajiaku, I.H.; Nikitin, A.; Sedlák, M.; Hutchinson, R.A.; Lacík, I. Radical polymerization of cationic methacrylate monomers TMAEMC and MAPTAC: Propagation rate coefficients obtained by PLP-SEC and batch polymerization. *Macromolecules* **2020**. manuscript in preparation.
27. Ezenwajiaku, I.H.; Chovancová, A.; Lister, K.; Lacík, I.; Hutchinson, R.A. Experimental and modeling investigation of radical homopolymerization of 2-(methacryloyloxyethyl) trimethylammonium chloride in aqueous solution. *Macromol. React. Eng.* **2020**, *14*. [CrossRef]
28. Cuccato, D.; Storti, G.; Morbidelli, M. Experimental and modeling study of acrylamide copolymerization with quaternary ammonium salt in aqueous solution. *Macromolecules* **2015**, *48*, 5076–5087. [CrossRef]
29. Ezenwajiaku, I.H.; Zigelstein, R.; Chovancová, A.; Lacík, I.; Hutchinson, R.A. Experimental and modeling investigations of aqueous-phase radical copolymerization of 2-(methacryloyloxyethyl)trimethylammonium chloride with acrylic acid. *Ind. Eng. Chem. Res.* **2020**, *59*, 3359–3374. [CrossRef]
30. Losada, R.; Wandrey, C. Copolymerization of a cationic double-charged monomer and electrochemical properties of the copolymers. *Macromolecules* **2009**, *42*, 3285–3293. [CrossRef]
31. Lacík, I.; Chovancová, A.; Uhelská, L.; Preusser, C.; Hutchinson, R.A.; Buback, M. PLP-SEC studies into the propagation rate coefficient of acrylamide radical polymerization in aqueous solution. *Macromolecules* **2016**, *49*, 3244–3253. [CrossRef]
32. Lacík, I.; Sobolčiak, P.; Stach, M.; Chorvát, D.; Kasák, P. Propagation rate coefficient for sulfobetaine monomers by PLP–SEC. *Polymer* **2016**, *87*, 38–49. [CrossRef]
33. Dobrynin, A.V.; Rubinstein, M. Theory of polyelectrolytes in solutions and at surfaces. *Prog. Polym. Sci.* **2005**, *30*, 1049–1118. [CrossRef]

34. Tanaka, H. Copolymerization of cationic monomers with acrylamide in an aqueous solution. *J. Polym. Sci. Part A Polym. Chem.* **1986**, *24*, 29–36. [CrossRef]
35. Hunkeler, D.; Hamielec, A.E.; Baade, W. The polymerization of quaternary ammonium cationic monomers with acrylamide. *Adv. Chem. Ser.* **1989**, *223*, 175–192.
36. McCormick, C.L.; Lowe, A.B.; Ayres, N. Water-soluble polymers. In *Kirk-Othmer Encyclopedia of Chemical Technology*, 5th ed.; Kroschwitz, J., Ed.; Wiley-Interscience: New York, NY, USA, 2001; Volume 20, pp. 435–504.
37. Drawe, P.; Kattner, H.; Buback, M. Kinetics and modeling of the radical polymerization of trimethylaminoethyl methacrylate chloride in aqueous solution. *Macromol. Chem. Phys.* **2016**, *217*, 2755–2764. [CrossRef]
38. Wako Speciality Chemicals Home Page. Available online: https://www.wakospecialtychemicals.com/brand/wako/product/v-50-azo-initiator/ (accessed on 15 February 2017).
39. Kattner, H. Radical Polymerization Kinetics of Nonionized and Fully Ionized Monomers Studied by Pulsed-Laser EPR. Ph.D. Thesis, Georg-August-Universität Göttingen, Göttingen, Germany, June 2016.
40. Smith, G.B.; Russell, G.T.; Heuts, J.P.A. Termination in dilute-solution free-radical polymerization: A composite model. *Macromol. Theory Sim.* **2003**, *12*, 299–314. [CrossRef]
41. Kazemi, N.; Duever, T.A.; Penlidis, A. Reactivity ratio estimation from cumulative copolymer composition data. *Macromol. React. Eng.* **2011**, *5*, 385–403. [CrossRef]
42. Preusser, C.; Hutchinson, R.A. An in situ NMR study of radical copolymerization kinetics of acrylamide and non-ionized acrylic acid in aqueous solution. *Macromol. Symp.* **2013**, *333*, 122–137. [CrossRef]

Publisher's Note: MDPI stays neutral with regard to jurisdictional claims in published maps and institutional affiliations.

© 2020 by the authors. Licensee MDPI, Basel, Switzerland. This article is an open access article distributed under the terms and conditions of the Creative Commons Attribution (CC BY) license (http://creativecommons.org/licenses/by/4.0/).